中國機械工程學刊第四十六卷第二期第 141~151 頁(民國一百一十四年)
Journal of the Chinese Society of Mechanical Engineers, Vol.46, No.2, pp 141~151 (2025)

Observational Modeling of Clutch Thermal Effects and Temperature Protection Prediction with Long and Short-Term Memory Network

Xiao-Hu Geng*, Wei-Dong Liu**and Yu-Long Lei**

Keywords： clutch thermal effects, temperature prediction, long and short-term memory network.

ABSTRACT

When an automatic mechanical transmission (AMT) shifts gears frequently, the clutch is repeatedly in the state of slipping, which makes the clutch thermal effects accumulate rapidly. The temperature in the frictional parts rises and spreads after the clutch's frictional work is applied, that needs some moments. To observe the clutch thermal effects and overcome the delay of temperature rise variation on clutch control, this paper proposes a prediction control for clutch temperature protection based on the long short-term memory (LSTM) network. Firstly, an extended state observation (ESO) model for clutch temperature based on clutch dynamics and heat transfer theory was established to estimate the temperature of the friction parts. Secondly, the future trend of clutch temperature was predicted based on the LSTM network algorithm, and the temperature was prevented from exceeding the threshold by adjusting the shift frequency and clutch input torque. Finally, the bench experiment was conducted to manipulate the AMT and clutch for 20 upshift and downshift cycles to compare the effect of temperature protection with LSTM and recurrent neural network (RNN) predictive control. The results shown the 16.21% reduction in high temperature operating time (over 250°C) with LSTM predictive control and the friction work was reduced from 5812.47kJ to 5380.48kJ.

INTRODUCTION

Repeated engagement in the dry clutch system leads to a significant increase in the temperature of the threshold range of 250°C to 300°C after prolonged slipping(Meng and Xi, 2021). Excessively high temperatures will result in a phenomenal decrease in the coefficient of friction, inadequate shift quality control, and potential clutch failure(Pisaturo and Senatore, 2019). Therefore, it is essential to investigate the temperature variation characteristics of friction components to effectively control the engagement of the clutch. Currently, the primary methods for characterizing clutch temperature are through finite element analysis (FEA), mathematical modeling, and experimental analysis(Jabbar et al., 2021).

The finite element approach is adopted to analyze the temperature of the clutch friction components by building an axisymmetric finite element model(Majeed et al., 2020). Researchers have used FEA software to analyze the variation of clutch temperature by varying the friction material (Sabri et al., 2021), engagement pressure (Stojanovic et al., 2020), sliding speed(Abdullah et al., 2020; Saffar et al., 2023), engagement conditions(Wu, 2021; Zhu et al., 2019) and so on. Computer simulation is used to simulate clutch engagement through FEA, but it is not feasible to estimate the clutch temperature online in real time according to the vehicle's powertrain conditions.

Mathematical modeling approach is used to evaluate the temperature of individual friction components by developing the mathematical model of clutch temperature based on principles of dynamics and heat transfer theory. During clutch slipping friction, the total heat quantity input is distributed according to the heat diffusion mathematical formula and the friction component temperature is estimated(Abdullah et al., 2018). The longer the duration of slipping friction when the clutch is engaged, the higher the temperature rise(Gkinis et al., 2018; Topczewska et al., 2020). At temperatures above the threshold range of 250~300°C, the decomposition of the clutch friction material leads to a sharp decrease in the coefficient of friction(Qiao et al., 2022). The thermoelastic instability of the clutch system worsens with time due to the accumulation of friction work. Therefore, studying the clutch thermal

Paper Received August, 2024. Revised December, 2024. Accepted December, 2024. Author for Correspondence: Xiao-Hu Geng.

* *Graduate Student, State Key Laboratory of Automotive Simulation and Control, Jilin University, Changchun, Jilin 130000, China.*

** *Professor, State Key Laboratory of Automotive Simulation and Control, Jilin University, Changchun, Jilin 130000, Chin.*

effect through the mathematical modeling is essential to enhance the torque transfer performance of automotive clutch (Della Gatta et al., 2018).

The experimental approach involves testing the clutch under various operating conditions on a bench or a vehicle, and collecting the clutch component temperatures through sensors(Skugor et al., 2020; Jin et al., 2022). The researchers have built a temperature model of the clutch based on processing and analyzing the data(Cakmak and Kilic, 2020). Direct temperature measurement of clutch friction parts is complex and costly, making it challenging to apply in vehicles. However, a bench can be constructed to simulate the actual vehicle driving environment, and mathematical modeling can be used to observe the clutch temperature.

The main contribution of this study lies in the following aspects. An experiment platform is built to simulate the real application environment of commercial vehicle clutch and to perform clutch temperature prediction control tests, as shown in Fig. 1. Data are collected online by a torque meter and a clutch position sensor. The temperature observation model of the clutch friction parts is established based on clutch dynamics and heat transfer theory. ESO is used to reduce the measurement perturbation and improve the temperature estimation accuracy. Prediction of future trends in clutch temperature with the help of deep LSTM network algorithm. If the forecast value surpasses the heat threshold of the clutch, the drive motor's torque output and AMT shift frequency will be anticipatedly regulated to impede the temperature from exceeding the threshold. This approach can be used in engineering practice to reduce clutch operating time at high temperatures, improve clutch performance and extend clutch life.

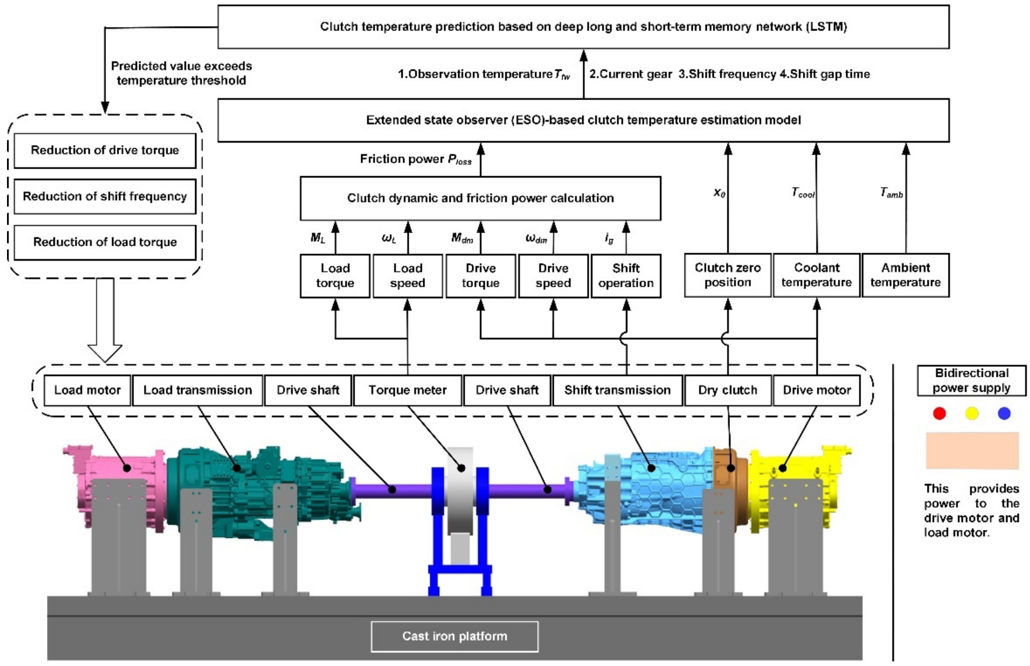

Fig. 1. Schematic diagram of the clutch temperature observation and protection experiment platform.

CLUTCH DYNAMICS ANALYSIS

During AMT gear shifting, clutch temperature is one of the key factors affecting the characteristics of dry clutches. On the one hand, the clutch temperature variation makes the clutch friction coefficient and torque transfer capability change (Myklebust and Eriksson, 2015), as shown in Fig. 2, which directly affects the control performance of AMT such as starting and shifting. On the other hand, clutch wear characteristics increase with increasing temperature, with the consequent decrease in clutch life, safety and reliability. Therefore, it is very meaningful to predict the clutch plate temperature by other easy-to-meter parameters, so as to optimize the AMT control design, increase the temperature warning, effectively control the temperature rise, and avoid overheating damage and thermal failure of the clutch in the process of starting and shifting.

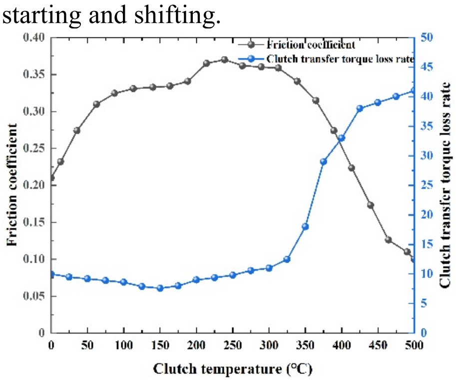

Fig. 2. Clutch temperature affects its operating characteristic.

AMT clutch have two modes: slipping mode and engagement mode. In the engagement mode, the clutch behaves as a rigid body, whereas in the slipping mode, the clutch consists of two parts: the master and the slave. The clutch enters the slipping friction phase and the kinetic equations for this process as follows:

$$\begin{aligned} J_D\dot{\omega}_{dm} &= M_{dm} - M_{cf} - b_D\omega_{dm} \\ J_L\dot{\omega}_{cf} &= M_{cf} - M_L - b_L\omega_{cf} \end{aligned} \tag{1}$$

where ω_{dm} is the drive motor output angular velocity, rad/s; ω_{cf} is the clutch friction plate angular velocity, rad/s; M_{dm} is the drive motor torque, Nm; M_{cf} is the clutch friction torque, Nm; M_L is the equivalent load torque at the clutch driven end, Nm, M_L=M_{tm}/i_g; i_g is shift transmission speed ratio; M_{tm} is the torque collected by the torque meter, Nm; J_D and b_D are the equivalent rotational inertia and damping coefficient of the clutch active end, kg·m^2 and N/(m/s); J_L and b_L are the equivalent rotational inertia and damping coefficient of the clutch load end, kg·m^2 and N/(m/s).

During the clutch engagement process, the experiment platform applies load to the clutch driven end through the load motor and load transmission to simulate the actual vehicle working load, and the load torque output from the loading device is collected by the torque meter. Therefore, the torque meter torque is M_{tm} = M_{lm}·i_l, M_{lm} is the load motor torque, Nm; i_l is load transmission speed ratio. The equivalent rotational inertia and damping coefficient as follows:

$$\begin{cases} J_D = J_{dm} + J_{fw} + J_{cl} \\ J_L = J_{st} + J_{ds} + J_{lt} + J_{lm} \\ b_D = b_{dm} + b_{fw} + b_{cl} \\ b_L = b_{st} + b_{ds} + b_{lt} + b_{lm} \end{cases} \tag{2}$$

where J_{dm} is the rotational inertia of the drive motor rotating parts, kg·m^2; J_{fw} is the flywheel rotational inertia, kg·m^2; J_{cl} is the clutch rotational inertia, kg·m^2; J_{st}, J_{ds}, J_{lt} and J_{lm} are the rotational inertia of the shift transmission, drive shaft, load transmission and load motor rotating parts, kg·m^2; b_{dm} is the drive motor rotating parts damping coefficient, N/(m/s); b_{fw} is the flywheel damping coefficient, N/(m/s); b_{cl} is the clutch damping coefficient, N/(m/s); b_{st}, b_{ds}, b_{lt} and b_{lm} are the damping coefficient of the shift transmission, drive shaft, load transmission and load motor rotating parts, N/(m/s).

When the clutch enters the synchronization phase, the torque output from the drive motor can be transferred to the shift transmission without loss, and the dynamic equations as follows:

$$\begin{cases} (J_D + J_L)\dot{\omega}_{cf} = M_{dm} - M_{cf} - (b_D + b_L)\omega_{cf} \\ \omega_{dm} = \omega_{cf} \end{cases} \tag{3}$$

After the clutch is engaged, the vehicle enters a stable driving state. The drive motor and AMT are considered as consolidated and the clutch system has no friction losses.

CLUTCH TEMPERATURE OBSERVATION MODEL

This section analyses the diffusion process of thermal effects in the clutch friction components. The clutch zero position x_0 of the clutch actuator is subject to position changes due to thermal expansion of the friction plates and can therefore be used as a means of observing the temperature rise of the clutch. The clutch temperature is then modeled so that it can be used in engineering applications that meet the development requirements. To reduce measurement disturbance in temperature and displacement sensor signals, an expanded state observer (ESO) is utilized to observe the temperature increase of the main clutch operating components, including the pressure plate and flywheel.

Temperature Effects Analysis

The friction work generated by clutch slipping is converted into heat and diffused through the pressure plate and flywheel. The pressure plate and flywheel initially absorb heat through frictional work surfaces. This heat is then conducted to the entire throughout pressure plate and flywheel, and subsequently diffused into the surrounding air and the clutch housing through convection and radiation. The transfer of heat causes an increase in temperature of the flywheel, the pressure plate, and other related parts. Schematic diagram of the heat dissipation path of the clutch slipping friction as shown in Fig. 3. Therefore, the temperature of the clutch is determined by the amount of friction work produced and the heat dissipation conditions of the transmission. These two factors have a combined effect on the temperature of the clutch.

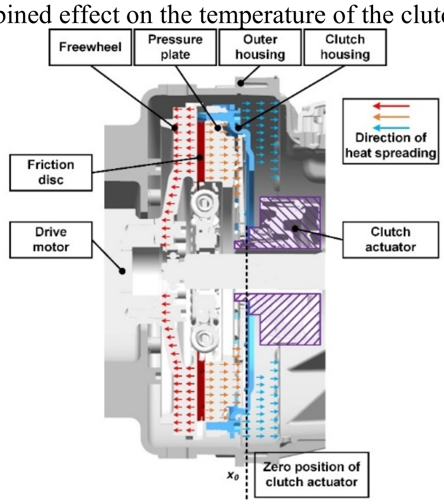

Fig. 3. Heat dissipation path of the clutch slipping.

In the clutch engagement process, friction power and friction work are the basis for measuring the thermal load.

$$P_{loss} = M_{cf}(\omega_{dm} - \omega_{cf}) \tag{4}$$

where P_{loss} is the clutch friction power, kW.

The friction disc is right in the middle and its heat spreads outwards through the flywheel and pressure plate. As the friction material of the clutch disc has poor heat absorption, the amount of heat absorbed is negligible compared to that absorbed by the pressure plate and flywheel. Therefore, this study only focuses on the absorption of heat generated by slipping friction by the clutch pressure plate and flywheel. When the clutch rotates at high speed, the clutch pressure plate, the flywheel, and the surrounding air move relative to each other at high speed. The heat balance equation(Myklebust and Eriksson, 2015) for the flywheel and pressure plate are as follows:

$$\dot{T}_{fw} = \frac{1}{m_{fw}c_p}[\alpha_{power}P_{loss} + k_{fw-pp}(T_{pp} - T_{fw}) + k_{fw-ch}(T_{ch} - T_{fw}) + k_{fw-oh}(T_{oh} - T_{fw}) + k_{fw-cool}(T_{cool} - T_{fw})] \tag{5}$$

$$\dot{T}_{pp} = \frac{1}{m_{pp}c_p}[(1-\alpha_{power})P_{loss} + k_{fw-pp}(T_{fw} - T_{pp}) + k_{pp-ch}(T_{ch} - T_{pp})] \tag{6}$$

where T_{fw}, T_{pp}, T_{ch}, T_{oh} and T_{cool} are the characteristic temperature of the flywheel, pressure plate, clutch housing, outer housing, and drive motor coolant, respectively, and the units are °C; α_{power} denotes heat distribution coefficient; $\alpha_{power}P_{loss}$ is the heat generated when the flywheel and friction discs rub against each other, kW; $(1-\alpha_{power})P_{loss}$ is the heat generated when the pressure plate and friction discs rub against each other, kW; m_{fw} and m_{pp} are the flywheel and pressure plate mass, kg; c_p is the specific heat capacity, J/(kg.℃).

Due to the poor heat absorption of air and the high-speed rotation of the clutch, it is assumed that the temperature inside the outer housing remains constant and any heat absorbed by the air is negligible. The heat generated inside the outer housing is dissipated through conduction and convection to the atmosphere. The heat balance equation for the clutch housing and outer housing are as follows:

$$\dot{T}_{ch} = \frac{1}{m_{ch}c_p}[k_{fw-ch}(T_{fw} - T_{ch}) + k_{pp-ch}(T_{pp} - T_{ch}) + k_{ch-oh}(T_{oh} - T_{ch})] \tag{7}$$

$$\dot{T}_{oh} = \frac{1}{m_{oh}c_p}[k_{fw-oh}(T_{fw} - T_{oh}) + k_{ch-oh}(T_{ch} - T_{oh}) + k_{oh-amb}(T_{amb} - T_{oh})] + f_T \tag{8}$$

where T_{amb} is the characteristic temperature of external atmospheric environment, °C; m_{ch} and m_{oh} are the mass of the clutch housing and outer housing, kg; k_{fw-pp}, k_{fw-ch}, k_{fw-oh}, $k_{fw-cool}$, k_{pp-ch}, k_{ch-oh}, and k_{oh-amb} are the heat dissipation factors between the components as shown in Table 1; f_T is a disturbance in the collection of information from the outer housing temperature sensor.

Testing reveals that the expansion of the clutch friction discs causes an offset in the zero position x_0 of the actuator. It is assumed that the expansion of the lever and clutch body is a linear function of temperature in order to establish a relationship between the temperature model and the change in zero position.

$$\dot{x}_0 = k_{\exp 1}(\frac{T_{fw} + T_{pp}}{2} - T_{amb}) + k_{\exp 2}(T_{pp} - T_{fw}) + f_x \tag{9}$$

where k_{exp1} and k_{exp2} are the expansion factors; f_x is a disturbance in the collection of information from the clutch actuator position sensor.

Table 1. Clutch temperature modeling parameters.

Parameters		Values
Heat distribution coefficient	α_{power}	0.78
Specific heat capacity	c_p	452.1 J/(kg.°C)
Flywheel mass	m_{fw}	40.63 kg
Pressure plate mass	m_{pp}	27.58 kg
Clutch housing mass	m_{ch}	9.32 kg
Outer housing mass	m_{oh}	29.14 kg
Heat dissipation factor between flywheel and pressure plate	k_{fw-pp}	10.12
Heat dissipation factor between flywheel and clutch housing	k_{fw-ch}	36.95
Heat dissipation factor between flywheel and outer housing	k_{fw-oh}	4.11
Heat dissipation factor between flywheel and drive motor	$k_{fw-cool}$	5.14
Heat dissipation factor between pressure plate and clutch housing	k_{pp-ch}	8.26
Heat dissipation factor between clutch housing and outer housing	k_{ch-oh}	52.32
Heat dissipation factor between outer housing and air environment	k_{oh-amb}	9.85
Expansion factor	k_{exp1}	13.82
Expansion factor	k_{exp2}	25.96

Temperature Extended State Observation Design

The temperature distribution of various clutch components, such as the pressure plate, flywheel, and housing can be calculated by analyzing the clutch's thermal effect. The sensors are capable to collect the temperature variable T_{oh} and the displacement variable x_0 for the mathematical model of the clutch thermal effect. Measuring the temperature variables T_{fw}, T_{pp} and T_{ch} for the friction component is challenging due to the high cost of sensor equipment and the difficulty in operating the collection process. Thus, a state space model of the clutch temperature is created using the system differential Equation (5) ~ (9), and a state observer is designed to estimate the unknown state variables of the system based on the known state variables.

The following definitions are made: state vector $X = [T_{fw}, T_{pp}, T_{ch}, T_{oh}, x_0]^T$, input vector $U = [P_{loss}]$, $P = [T_{cool}, T_{amb}]^T$, $F = [f_T, f_x]^T$ and output vector $Y = [T_{fw}, x_0]^T$. Where P is available and F is perturbed. Now, the clutch temperature state-space model can be expressed as:

$$\begin{aligned} \dot{X} &= AX + B_uU + B_pP + B_fF \\ Y &= CX \end{aligned} \tag{10}$$

$$B_u = \begin{bmatrix} \alpha_{power} \\ 1-\alpha_{power} \\ 0 \\ 0 \\ 0 \end{bmatrix} \quad B_p = \begin{bmatrix} k_{fw-cool} & 0 \\ 0 & 0 \\ 0 & 0 \\ 0 & k_{oh-amb} \\ 0 & \frac{k_{\exp 1}}{2} \end{bmatrix} \quad B_f = \begin{bmatrix} 0 & 0 \\ 0 & 0 \\ 0 & 0 \\ 1 & 0 \\ 0 & 1 \end{bmatrix} \tag{11}$$

$$A=\begin{bmatrix} \frac{-(k_{fw-pp}+k_{fw-ch}+k_{fw-oh}+k_{fw-cool})}{m_{fw}c_p} & \frac{k_{fw-pp}}{m_{fw}c_p} & \frac{k_{fw-ch}}{m_{fw}c_p} & \frac{k_{fw-oh}}{m_{fw}c_p} & 0 \\ \frac{k_{fw-pp}}{m_{pp}c_p} & \frac{-(k_{fw-pp}+k_{pp-ch})}{m_{pp}c_p} & \frac{k_{pp-ch}}{m_{pp}c_p} & 0 & 0 \\ \frac{k_{fw-ch}}{m_{ch}c_p} & \frac{k_{pp-ch}}{m_{ch}c_p} & \frac{-(k_{fw-ch}+k_{pp-ch}+k_{ch-oh})}{m_{ch}c_p} & \frac{k_{ch-oh}}{m_{ch}c_p} & 0 \\ \frac{k_{fw-oh}}{m_{oh}c_p} & 0 & \frac{k_{ch-oh}}{m_{oh}c_p} & \frac{-(k_{fw-oh}+k_{ch-oh}+k_{oh-amb})}{m_{oh}c_p} & 0 \\ \frac{k_{\exp 1}}{2}-k_{\exp 2} & \frac{k_{\exp 1}}{2}+k_{\exp 2} & 0 & 0 & 0 \end{bmatrix} \quad (12)$$

$$C=[0,\ 0,\ 1,\ 0,\ 0;\ 0,\ 0,\ 0,\ 1,\ 0] \quad (13)$$

where A is the state matrix as shown in Equation (12). B_u, B_p and B_f are the coefficient matrices of the control variables, known variables and disturbance variables as shown in Equation (11). C is the output matrix as shown in Equation (13).

Since the measurement of system output variables is affected by random perturbations, in order to improve the accuracy of state variable observations. Therefore, ESO is used to observe this part of the perturbation and the ESO parameters are adjusted according to the results of the perturbation observation(Zhou and Chang, 2017). The system state reconstruction of the system space Equation (10) is performed to obtain the ESO equations as shown in Equation (14). The clutch temperature estimation model based on the ESO is shown in Fig. 4.

$$\begin{cases} \dot{\hat{X}}_1 = A_{1i}\hat{X}_i + B_{u,1}U + B_{P,1j}P_j + \frac{\alpha_1}{\varepsilon}(Y_1-\hat{Y}_1) \\ \dot{\hat{X}}_2 = A_{2i}\hat{X}_i + B_{u,2}U + B_{P,2j}P_j + \frac{\alpha_2}{\varepsilon}(Y_1-\hat{Y}_1) \\ \dot{\hat{X}}_3 = A_{3i}\hat{X}_i + B_{u,3}U + B_{P,3j}P_j + \frac{\alpha_3}{\varepsilon}(Y_1-\hat{Y}_1) \\ \dot{\hat{X}}_4 = \hat{\sigma}_1 + B_{u,4}U + B_{P,4j}P_j + \frac{\alpha_4}{\varepsilon}(Y_1-\hat{Y}_1) \\ \dot{\hat{X}}_5 = \hat{\sigma}_2 + B_{u,5}U + B_{P,5j}P_j + \frac{\alpha_5}{\varepsilon}(Y_2-\hat{Y}_2) \\ \dot{\hat{\sigma}}_1 = \frac{\alpha_6}{\varepsilon^2}(Y_1-\hat{Y}_1) \\ \dot{\hat{\sigma}}_2 = \frac{\alpha_7}{\varepsilon^2}(Y_2-\hat{Y}_2) \end{cases} \quad (14)$$

where $\hat{X}_{1\sim5}$ and $\hat{\sigma}_{1,2}$ are the observer state variables; $\hat{Y}_1$ and $\hat{Y}_2$ are the observer output variables; $\hat{\alpha}_{1\sim7}$ are positive real numbers; $\sigma>0$ and i =1, 2, ⋯, 5, j=1, 2.

The shift transmission underwent the cyclic shift test, during which the clutch is repeatedly engaged and disengaged, causing the temperature of the friction parts to rise and then cool. The zero position has been recorded as a measure of friction disc expansion. The variation of clutch zero position offset during temperature rise is shown in Fig. 5. As the clutch temperature increases, the more the friction discs expand and the greater the clutch zero position offset. Then the clutch cools and the clutch zero position bias decreases. The temperature model Equation (9) demonstrates a strong correlation with the measurements.

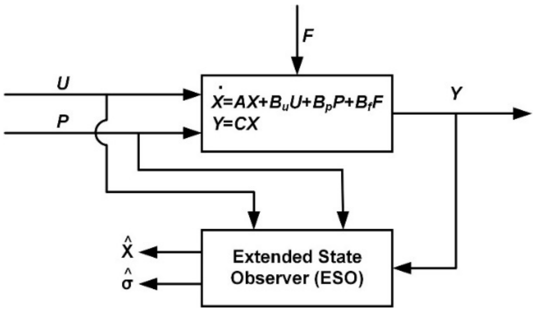

Fig. 4. Clutch temperature model based on ESO.

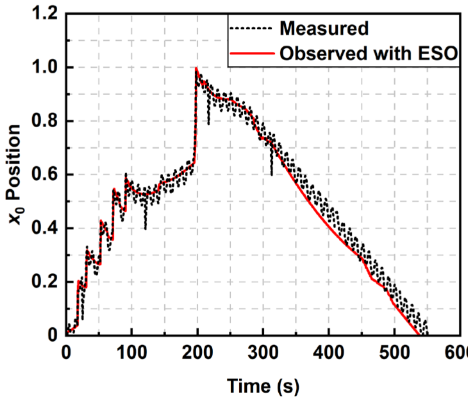

Fig. 5. Zero position x_0 measurement and thermal expansion observation of friction disc.

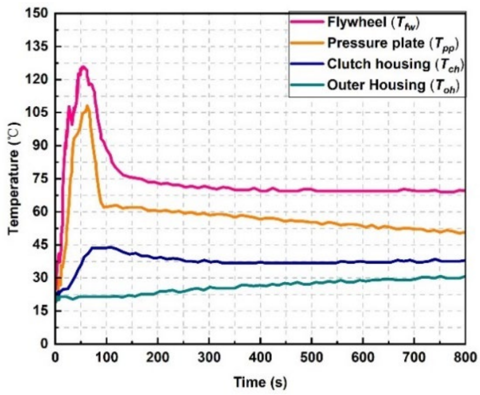

Fig. 6. Temperature variations of flywheel, pressure plate, clutch housing, and external housing.

The transmission gears shift continuously from 1st to 12th gear and then back down to 1st gear, constituting a shift cycle. During this process, the clutch is repeatedly engaged and disengaged, and the temperature change of the friction parts is observed, as shown in Fig. 6. The flywheel absorbs the most heat during clutch slipping. Therefore, the flywheel temperature T_{fw} is used to represent the clutch temperature. Next, effective measures are taken in advance to prevent the clutch temperature from exceeding the set threshold value by predicting the flywheel temperature T_{fw}.

DEEP LSTM-BASED CLUTCH TEMPERATURE PREDICTION

In this section, based on the current status of the clutch system, the LSTM algorithm is applied to the clutch temperature to predict its future trend. The temperature information that has been forecast is sent to the clutch control module. The clutch control module can adjust the control strategy in advance to prevent the clutch temperature from exceeding the threshold. This ensures the normal working performance of the AMT system and extends the service life of the clutch.

The Structure of the Deep LSTM

The deep neural network is capable of extracting abstract features hidden in vast amounts of data through multi-layer non-linear mapping(Mo et al., 2023).

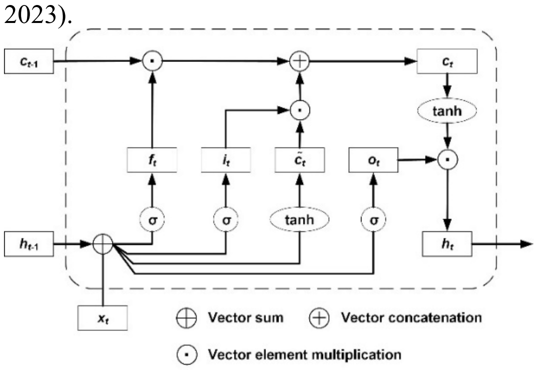

Fig. 7. Recurrent unit structure of the LSTM.

The structure of the LSTM unit is shown in Fig. 7. Each memory cell contains three types of "gate" structures: the input gate (i_t), the forget gate (f_t) and the output gate (o_t).

$$\begin{cases} i_t = \sigma(W_i x_t + U_i h_{t-1} + b_i) \\ f_t = \sigma(W_f x_t + U_f h_{t-1} + b_f) \\ o_t = \sigma(W_o x_t + U_o h_{t-1} + b_o) \end{cases} \tag{15}$$

where $\sigma(\cdot)$ is the Logistic function with output interval (0,1); x_t is the input at the current moment; $h_{t\text{-}1}$ is the hidden state at the previous moment; W_i, W_f, and W_o are the state-input weighs; U_i, U_f, and U_o are the state-state weights; b_i, b_f, and b_o are the biases.

The LSTM network introduces a new internal state c_t (the cell state) dedicated to linear cyclic message passing, while nonlinearly outputting information to the hidden layer external variable h_t (the hidden state). To obtain the candidate function $\tilde{c}_t$ (the cell candidate state) by means of the nonlinear function.

$$\begin{cases} c_t = f_t \otimes c_{t-1} + i_t \otimes \tilde{c}_t \\ h_t = o_t \otimes \tanh(c_t) \\ \tilde{c}_t = \tanh(W_{\tilde{c}} x_t + U_{\tilde{c}} h_{t-1} + b_{\tilde{c}}) \end{cases} \tag{16}$$

where tanh denotes the activation function and $\otimes$ denotes the vector element product; $W_{\tilde{c}}$ and $U_{\tilde{c}}$ are the weights; $b_{\tilde{c}}$ is the bias.

At the output layer, an activation function is used in order to obtain the final output signal. The predicted value $\hat{y}$ as follows:

$$\hat{y}_i = \sigma(z_i) = \sigma(W_z h_t + b_z) \tag{17}$$

The architecture of the deep LSTM network consists of a LSTM layer, a fully connected (FC) layer and an output layer (in the Fig. 8), and shows excellent capabilities in processing time series data used for prediction and regression problems.

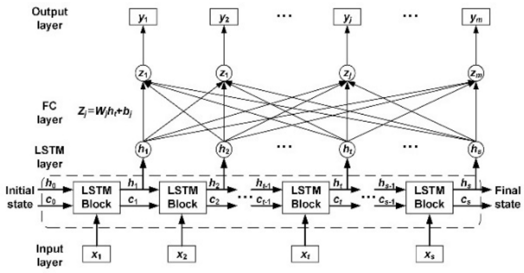

Fig. 8. Architecture of the deep LSTM.

Clutch Temperature Prediction

The approach to predicting the clutch temperature is shown in Fig. 9. To predict the clutch temperature, historical observations of the clutch temperature, current gear, shift frequency, and shift gap time are necessary.

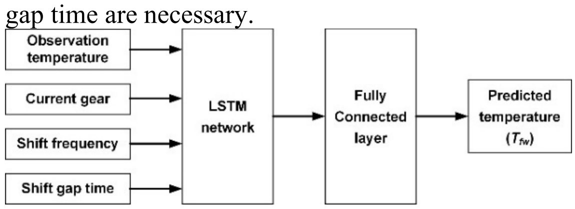

Fig. 9. The schematic of the deep LSTM based clutch temperature prediction.

Clutch temperature observation T_{fw} is obtained via ESO. For shift transmission, the current gear position is obtained by the gear displacement sensor and then the frequency of gear change is obtained by statistical calculation. The shift gap time is the time it takes for the shift transmission to change from one gear to another. In Fig. 10, it can be seen that the shift transmission is continuously upgraded from 5th gear to 11th gear, and the shift gap time are 750ms, 842ms, 853ms, 935ms, 854ms, and 874ms, respectively. The longer the shift gap time is, the longer the clutch slipping process is, and the larger the slipping work is, and the faster the clutch temperature rises.

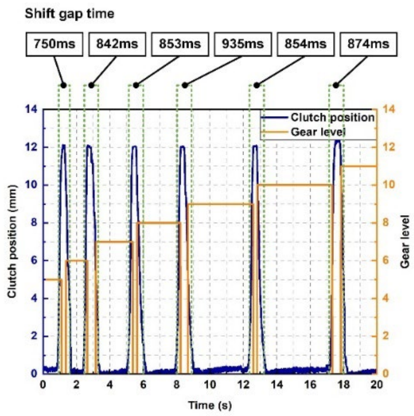

Fig. 10. Clutch position, current gear and shift time.

When performing clutch temperature prediction, the selection of the prediction steps also has a large impact on the accuracy and real-time performance of the control. The suitable prediction steps will be able to accurately predict the development of changes in the system behavior and provide enough prediction time for the LSTM control to act as an override control.

The prediction steps are related to the time lag, to the sampling period, to the number of model dimensions, and to the rate of change of the system output. Therefore, the selection of the prediction steps is specifically determined in the experimental debugging. In the clutch control task, the clutch temperature prediction is a 50ms calculation task. The LSTM temperature calculation module outputs the calculation result every 50ms according to the input information (the step is 50ms). The prediction steps are selected as 10, 20 and 30, respectively, and the results of the clutch temperature prediction are shown in Fig. 11(a), (b),and (c),.

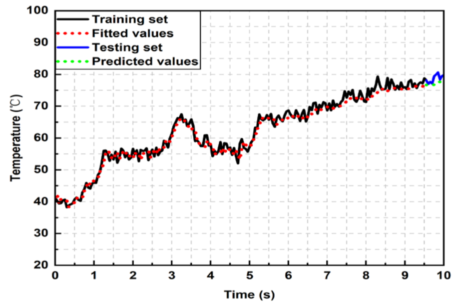

(a) prediction steps of 10

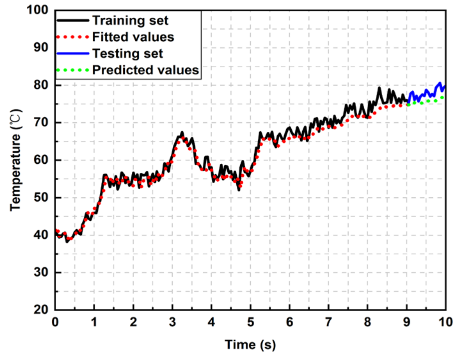

(b) prediction steps of 20

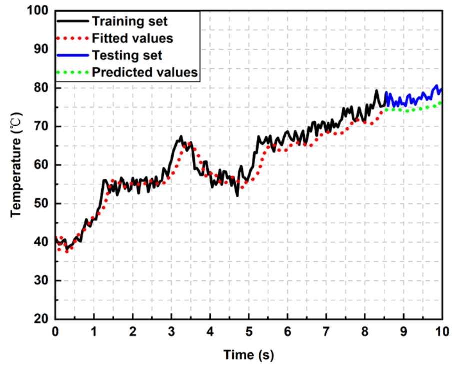

(c) prediction steps of 30

Fig. 11. LSTM-based clutch temperature prediction results.

In this study, both clutch temperature prediction accuracy and adequate prediction trends are considered. The clutch shift gap is in the range of 500ms ~ 1000ms, which is equivalent to 10 ~ 20 steps. In order to the clutch temperature prediction to guide the override control of the shift, the clutch temperature prediction time should be greater than 1000ms (20 steps). However, when the prediction time exceeds 25 steps, the temperature prediction accuracy decreases rapidly as shown in Table 2. Therefore, the prediction steps are determined to be 20 steps.

Table 2. Clutch prediction accuracy at different steps.

Predicted steps	RMSE	MEA	R^2
5 steps	2.802	1.093	0.9583
10 steps	3.147	2.352	0.9475
15 steps	3.462	2.527	0.9366
20 steps	3.853	2.848	0.9016
25 steps	7.745	5.263	0.8747
30 steps	9.291	8.013	0.8072

Clutch High Temperature Prevention

The basic idea of LSTM predictive control of clutch temperature is shown in Fig. 12.

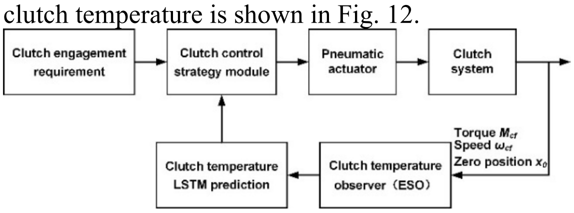

Fig. 12. LSTM-based clutch temperature predictive control principle.

The clutch temperature trend is shown in Fig. 13(a), the corresponding Fig. 13(b) shows the torque adjustment strategy, and the corresponding Fig. 13(c) shows the shift frequency adjustment strategy.

(1) If the clutch temperature as shown in the two cases of [1] and [2] in Fig. 13(a), the temperature is in the decline, or rise slower and from the temperature threshold value of 250 ℃ value of a large gap. The clutch torque can be determined by following strategy [A] in Fig. 13(b), while maintaining the transmission shift frequency in state [D] as shown in Fig. 13(c).

(2) If the clutch temperature increase follows the trend [3] shown in Fig. 13(a), the clutch torque can be

corrected accordingly using the strategy [B] in Fig. 13(b), while changing the frequency of transmission shifts to the [E] state as shown in Fig. 13(c).

(3) If the temperature trend of the clutch follows the behavior [4] in Fig. 13(a), the temperature will rise rapidly. To prevent this, the clutch torque should be significantly reduced beforehand, as demonstrated in strategy [C] in Fig. 13(b). Additionally, the frequency of transmission shifts should be decreased to minimize clutch slipping time, as demonstrated in strategy [F] in Fig. 13(c).

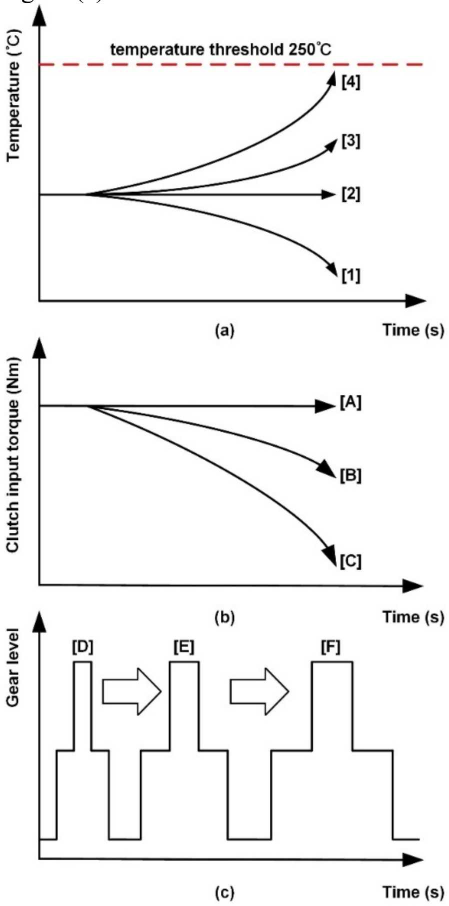

Fig. 13. Clutch high temperature prevention strategy.

The advantage of the prediction control strategy is that the system can correct the clutch input torque and shift frequency in advance according to the predicted future development trend of the clutch temperature, and the magnitude of the correction can be decided according to the predicted rate of temperature rise.

EXPERIMENT RESULTS AND DISCUSSIONS

Experimental Steup

To verify the validity of the clutch thermal effect model and temperature prediction protection strategy proposed in this paper, cyclic shifting of the AMT was performed on the bench with the clutch working in conjunction, as shown in Fig. 14. The main parameters of the experimental platform equipment were shown in Table 3. The clutch input shaft is driven by a high-power permanent magnet synchronous motor (peak power is 360kW and peak torque is 2,500Nm), and the output shaft is connected to the shift transmission (with 12 speed ratios). The load torque is reconstructed from the torque measured by the torque sensor mounted between the shift transmission and the load transmission, as well as the sensor's torque range of 0±50000Nm and speed range of 0~3000rpm, and the sensor accuracy is 0.1%. Load resistance to the experiment platform is provided by the load motor and load transmission.

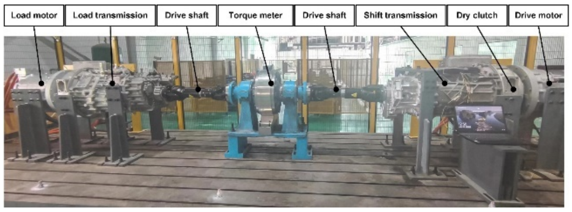

Fig. 14. Experiment platform actual scene diagram.

Table 3. The parameters of the platform equipment.

Equipment name	Parameters	Values
Drive motor and load motor (Both are the same model number)	Type	Permanent magnetic synchronization
	Rated power	250 kW
	Peak power	360 kW
	Rated torque	1400 Nm
	Peak torque	2500 Nm
	Rated speed	1700 rpm
	Peak speed	3000 rpm
Dry clutch	Torque capacity	3000 Nm
	Reserve factor	1.2
Shift transmission	Number of gears	12
Torque meter	Torque range	0±50000 Nm
	Speed range	0~3000 rpm
Load transmission	Number of gears	12

The number of transmission shift cycles was set to 20 times. In each shift cycle, the gears were sequentially raised from 1 up to 12, and then lowered from 12 to 1. The clutch repeatedly engaged, slipped, and disengaged during the gearshift cycle of the transmission.

Results and Discussion

The experimental results of the with recurrent neural network (RNN) clutch temperature prediction protection were shown in Fig. 15. The time taken after 20 rounds of shifting was 2875s and the average temperature was 179.66°C. The clutch temperature reached the threshold temperature of 250°C at 1932s, as shown in Fig. 15(a), at which time the shift transmission was in the 15th round of shifting. The clutch high temperature (above threshold temperature 250°C) operating time was 691 s. After the temperature reached the threshold value 250°C, the clutch torque started to decrease after 2100 s as shown in Fig. 15(b). Transmission shift frequency (in Fig. 15(c)) started to decrease after 2100 s, and clutch temperature started to stop increasing and decreased slightly.

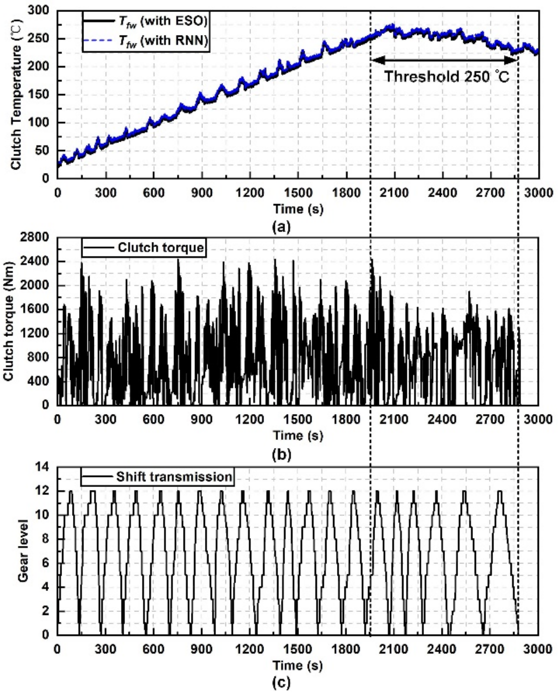

Fig. 15. The experimental results of the with RNN clutch temperature prediction protection.

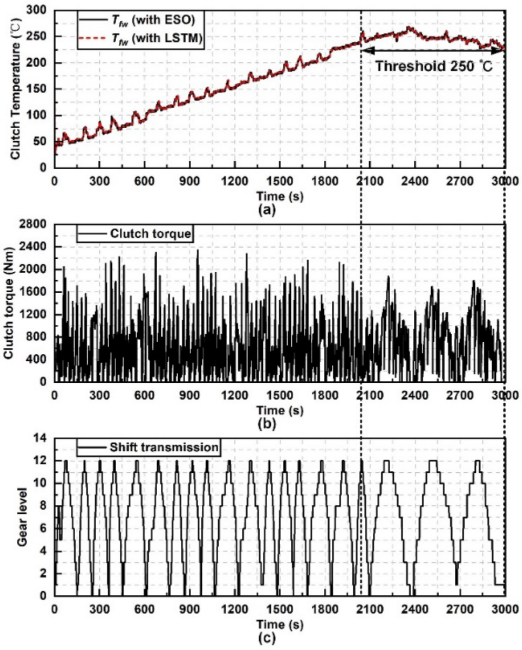

Fig. 16. The experimental results of the with LSTM clutch temperature prediction protection.

The experimental results of the with LSTM clutch temperature prediction protection were shown in Fig. 16. The time taken after 20 rounds of shifting was 3000 s and the average temperature was 174.11°C. The clutch temperature reached the threshold temperature of 250°C at 2042 s, as shown in Fig. 16(a), when the shift transmission was in its 17th shift cycle. The clutch high temperature (above 250°C) operating time was 579 s. The average shift cycle time for the previous 17 rounds was 123.5 s. After 2100 s, the shift cycle time become longer, with the 18th, 19th, and 20th shift cycle times averaging 300 s. In the 18th~20th rounds, the shift cycle time increased by 142.9%. After the temperature reached the threshold 250°C, the clutch torque started to decrease after 2100 s as shown in Fig. 16(b), and the frequency of gearshift of the transmission started to decrease at 2100 s as shown in Fig. 16(c). The temperature maintained a decreasing trend from 2100 s to 3000 s.

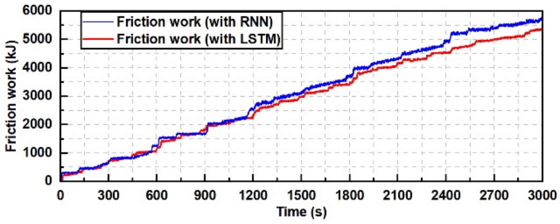

Fig. 17. Comparison results of friction work.

By comparing the results of Fig. 15 and Fig. 16, the following benefits could be obtained by using LSTM algorithm based clutch temperature prediction protection control, compared to the RNN network. During these 20 shift cycles, the average clutch temperature was reduced by 3.09% and the overall clutch cooling problem was improved. Clutch high-temperature (250°C or more) operation time was reduced by 16.21%, which effectively prevents high-temperature clutch failures. During another 20 rounds of gear changes, the time was extended by 4.35%, and the overall clutch usage time was improved. Meanwhile, the results of Fig. 17 shown that the slipping friction work decreased from 5812.47kJ to 5380.48kJ by adopting LSTM-based clutch temperature prediction protection approach, which was a decrease of 7.43%. Therefore, using the LSTM-based clutch temperature prediction and protection strategy proposed in this paper improved the control performance and service life of the automatic clutch.

CONCLUSIONS

In this paper, the clutch temperature diffusion process is analyzed and it is found that the flywheel absorbs the most heat. The flywheel characterization temperature is used to represent the clutch temperature. The LSTM algorithm is used to predict the future trend of clutch temperature, and the clutch control strategy is adjusted in advance to prevent the clutch temperature from exceeding the set threshold. The main conclusions as follows:

(1) An experiment platform is constructed to replicate the actual commercial vehicle clutch environment. The ESO temperature model, designed based on the clutch heat diffusion principle, can estimate the clutch temperature accurately and resist sensor measurement interference effectively.

(2) The clutch temperature trend can be effectively predicted based on the LSTM algorithm. This guarantees prediction accuracy (R^2>0.9) and sufficiently long time (with 1000ms) prediction

information under the 20 steps condition.

(3) The input torque of the clutch and the frequency of AMT shifts are adjusted in advance based on predicted temperatures. Compared with the RNN network, the use of the LSTM-based temperature prediction and protection strategy results in the 16.21% reduction in the operating time of the clutch at high temperatures (above 250°C), which improves the performance of automatic clutch control and extends its service life.

ACKNOWLEDGMENT

Financial support for this work was provided by the Sichuan Provincial Science and Technology Project "Research and Application of Key Technology of Multi-Gear Electric Drive System for Electric Heavy Trucks" (2023YFG0068).

REFERENCES

Abdullah, O. I., Schlattman, J., Majeed, M. H. and Sabri, L. A., "The temperatures distributions of a single-disc clutches using heat partitioning and total heat generated approaches," *Case Stud Therm Eng*, Vol. 11, No., pp. 43-54(2018).

Abdullah, O. I., Schlattmann, J., Senatore, A., Sabri, L. A. and Abd Al-Sahb, W. S., "Effect of Sliding Speed on the Thermal Stresses of Single-Disk Friction Clutches," *J Fail Anal Prev*, Vol. 20, No. 5, pp. 1534-1540(2020).

Cakmak, T. and Kilic, M., "Estimation of friction surface temperature of a dry clutch," *Int J Heavy Veh Syst*, Vol. 27, No. 5, pp. 683-702(2020).

Della Gatta, A., Iannelli, L., Pisaturo, M., Senatore, A. and Vasca, F., "A Dry Clutch Engagement Controller with Thermal Effects Compensation," *2018 Ieee Conference on Control Technology and Applications (Ccta)*, Vol. No., pp. 1228-1233(2018).

Gkinis, T., Rahmani, R., Rahnejat, H. and O'mahony, M., "Heat generation and transfer in automotive dry clutch engagement," *J Zhejiang Univ-Sc A*, Vol. 19, No. 3, pp. 175-188(2018).

Jabbar, N. A., Hussain, I. Y. and Abdullah, O. I., "Thermal and thermoelastic problems in dry friction clutch: A comprehensive review," *Heat Transfer*, Vol. 50, No. 8, pp. 7855-7878(2021).

Jin, Y. C., Chen, L. and Cheng, C., "Thermal behavior of friction discs in dry clutches based on a non-uniform pressure model," *Case Stud Therm Eng*, Vol. 32, No., (2022).

Majeed, M. H., Kadhim, D. E., Abdullah, O. and Schlattmann, J., "Numerical analysis of thermal problem in dry friction clutches based on the interactive design approach," *Int J Interact Des M*, Vol. 14, No. 3, pp. 1091-1101(2020).

Meng, F. and Xi, J. Q., "Numerical and Experimental Investigation of Temperature Distribution for Dry-Clutches," *Machines*, Vol. 9, No. 9, (2021).

Mo, J. C., Qin, D. T. and Liu, Y. G., "Fault Detection Strategy for Fork Displacement Sensor in Dual Clutch Transmission via Deep Long Short-Term Memory Network," *Ieee T Veh Technol*, Vol. 72, No. 7, pp. 8636-8646(2023).

Myklebust, A. and Eriksson, L., "Modeling, Observability, and Estimation of Thermal Effects and Aging on Transmitted Torque in a Heavy Duty Truck With a Dry Clutch," *Ieee-Asme T Mech*, Vol. 20, No. 1, pp. 61-72(2015).

Pisaturo, M. and Senatore, A., "Thermal Compensation Control Strategy in Automated Dry Clutch Engagement Dynamics and Launch Manoeuvre," *Int J Auto Tech-Kor*, Vol. 20, No. 6, pp. 1089-1101(2019).

Qiao, Y. J., Yi, Y. B., Wang, T., Cui, H. W. and Lian, Z. S., "Effect of Wear on Thermoelastic Instability Involving Friction Pair Thickness in Automotive Clutches," *Journal of Tribology-Tr ansactions of the Asme*, Vol. 144, No. 4, (2022).

Sabri, L. A., Stojanovic, N., Senatore, A., Jweeg, M. J., Abed, A. M. and Abdullah, O. I., "Three-Dimensional Finite Element Analysis of Contact Problem in Dry Friction Clutches," *Lubricants*, Vol. 9, No. 12, (2021).

Saffar, I. Q. A., Sultan, H. S., Jweeg, M. J., Abed, A. M., Abdullah, O. I., Schlattmann, J., Sabri, L. A. and Alfilh, R. H. C., "Investigation of the Influence of Sliding Speed on Thermoelastic Problem in the Frictional Clutch System When Applying a Constant Heat Generation," *Heat Transf Res*, Vol. 54, No. 7, pp. 19-40(2023).

Skugor, B., Deur, J. and Ivanovic, V., "E-Clutch Torque Control Including Compensation of Thermal Expansion Effects," *Ieee T Veh Technol*, Vol. 69, No. 1, pp. 246-257(2020).

Stojanovic, N., Abdullah, O. I., Rakisheva, Z. B., Lattieff, F. A. and Hashim, E. T., "The Effect of Applied Pressure Function on Thermo-elastic Problem in the Dry Friction Clutches," *J Fail Anal Prev*, Vol. 20, No. 6, pp. 2145-2152(2020).

Topczewska, K. A., Schlattmann, J. and Abdullah, O. I., "Temperature and Thermal Stresses Distributions in a Dry Friction Clutch," *J Theor App Mech-Pol*, Vol. 58, No. 2, pp. 351-360 (2020).

Wu, B., "Numerical Investigation of the Transient Temperature Field of a Dry Clutch Based on Starting Conditions," *J Appl Mech Tech Ph+*, Vol. 62, No. 2, pp. 283-291(2021).

Zhou, Y. C. and Chang, S. Q., "A Model-Assisted Reduced-Order ESO Based Cascade Controller for Sensorless Control of Independent Gear-Shifting Actuators," *Appl Sci-Basel*, Vol. 7, No. 12, (2017).

Zhu, M. T., Yao, P., Pu, Y. B. and Liu, T., "Comparative Study on the Temperature Rise of a Dry Dual Clutch Under Different Starting Conditions," *Automotive Innov*, Vol. 2, No. 1, pp. 35-44(2019).

離合器熱效應的觀測建模及基於長短期記憶網絡的溫度預測保護控制

耿小虎　　劉衛東　　雷玉龍
吉林大學汽車模擬與控制國家重點實驗室

摘 要

當自動機械變速器（AMT）頻繁換檔時，離合器反復處於打滑狀態會造成離合器熱效應迅速累積。在離合器施加摩擦功後，摩擦部件的溫度升高和擴散需要一定時間。為了觀察離合器熱效應並克服離合器控制中溫昇變化的延遲，本文提出了一種基於長短期記憶（LSTM）網絡的離合器溫度保護預測控制。首先，基於離合器動力學和傳熱理論建立了離合器溫度的擴展狀態觀測（ESO）模型，以估計摩擦部件的溫度。其次，基於 LSTM 網絡算瀌預測離合器溫度的未來趨勢，通過調整換檔頻率和離合器輸入扭矩來防止溫度超過閾值。最後，進行了臺架實驗，操縱 AMT 和離合器進行 20 個昇檔和降檔迴圈，比較了 LSTM 和迴圈神經網路（RNN）預測控制的溫度保護效果。 結果表明，採用 LSTM 預測控制，高溫運行時間(超過 250˚C)減少了 16.21%，摩擦功從 5812.47kJ 減少到 5380.48kJ。